Supplementary Information for

Shear-Controlled Composite Cathodes for All-Solid-State Batteries Combined Synergistically with Stereology-Driven Image Analysis

Hyeseong Jeong,[ab] Heesu Hwang,[c] Jeong-Won Cho,[c] Dongwook Shin,[b] Jong-Ho Lee,[a] Sung Soo Shin,*[d] Jin-Ha Hwang,*[c] and Hyoungchul Kim*[e]

[a]*Energy Materials Research Center, Korea Institute of Science and Technology, 5 Hwarang-ro 14-gil, Seongbuk-gu, Seoul 02792, Republic of Korea*

[b]*Division of Materials Science and Engineering, Hanyang University, 222 Wangsimni-ro, Seongdong-gu, Seoul 04763, Republic of Korea*

[c]*Department of Materials Science and Engineering, Hongik University, 94 Wausan-ro, Mapo-gu, Seoul 04066, Republic of Korea*

[d]*Department of Mechanical Engineering, Incheon National University, 199 Academy-ro, Yeonsu-gu, Incheon 22012, Republic of Korea*

[e]*Department of Mechanical and System Design Engineering, Hongik University, 94 Wausan-ro, Mapo-gu, Seoul 04066, Republic of Korea*

*Corresponding authors. E-mail address: ssshin@inu.ac.kr (S.S. Shin), jhwang@hongik.ac.kr (J.-H. Hwang), hyoungchul@hongik.ac.kr (H. Kim)

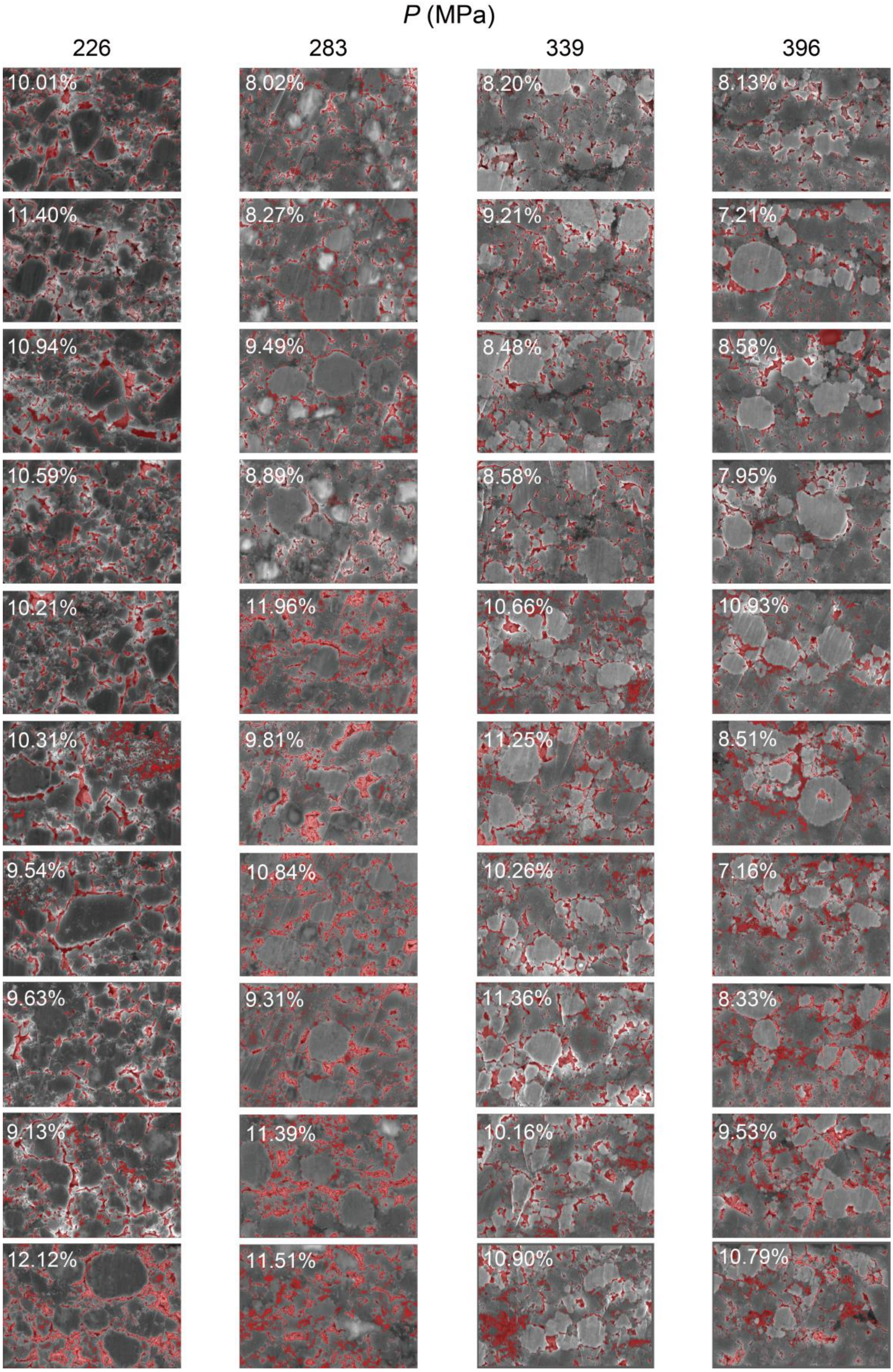

Fig. S1. Pore analysis of the as-fabricated composite cathode of free-to-uniaxial pressed cells (FUPCs). The graph illustrates porosity as a function of pressure (*P*), with the red colour indicating pore regions.

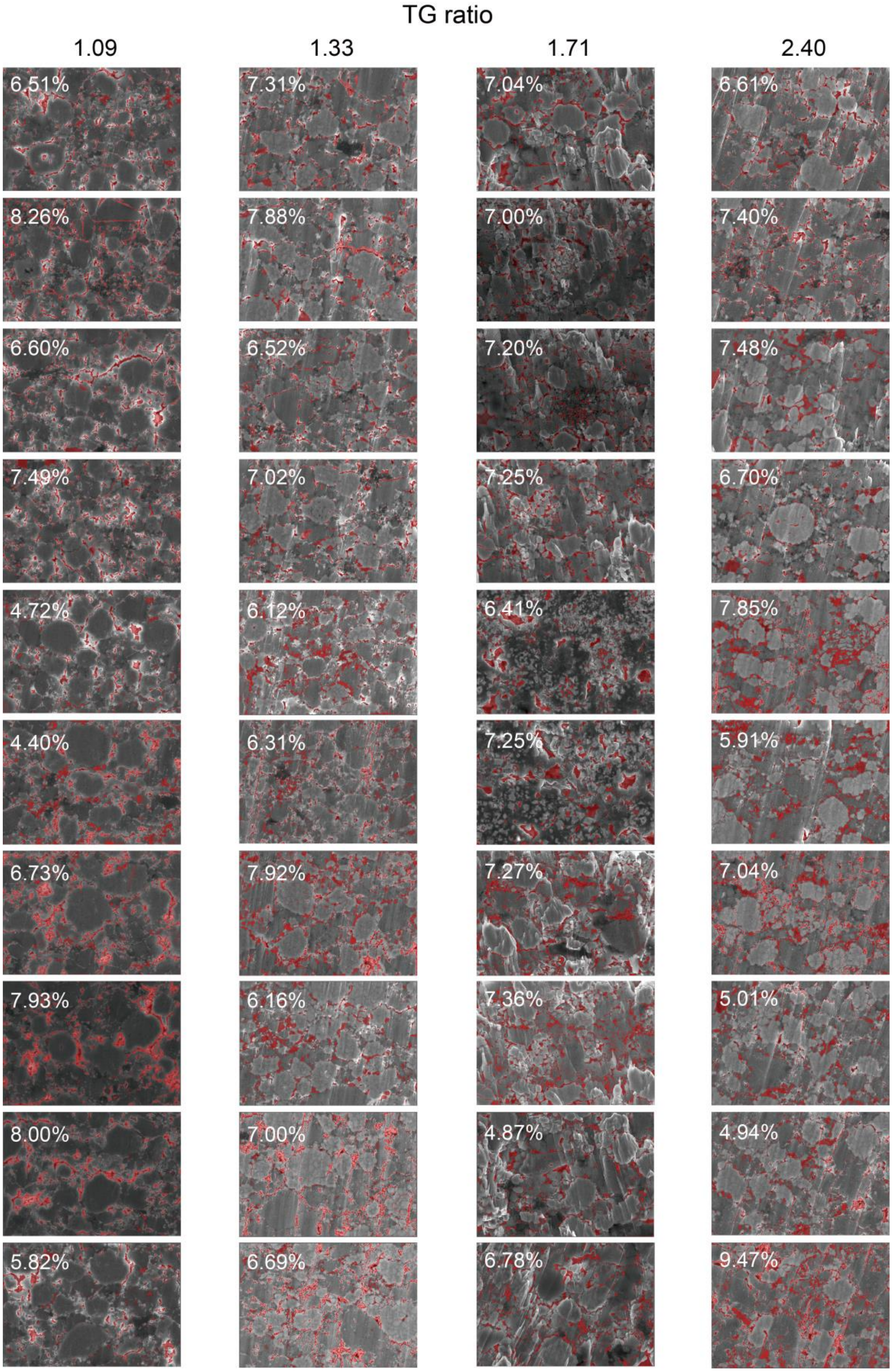

Fig. S2. Pore analysis of the as-fabricated composite cathode of roll-to-uniaxial pressed cells (RUPCs). The graph illustrates porosity as a function of thickness-to-gap (TG) ratio, with the red colour indicating pore regions.

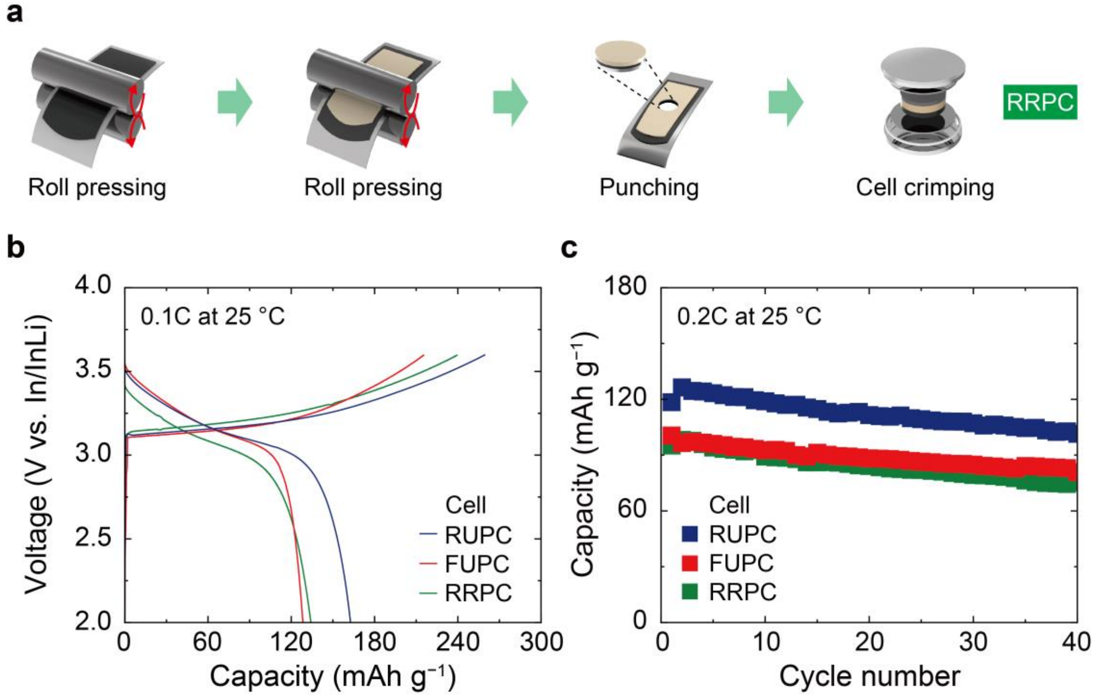

Fig. S3. Fabrication process and electrochemical performance of a reference roll-to-roll pressed cells (RRPC). (a) Depiction of cell fabrication processes using roll-to-roll pressing techniques. (b) Initial specific charge-discharge curves of the various cell types (RUPC, FUPC, and RRPC) at 0.1C. (c) Specific discharge capacities of the various cell types over 40 cycles at 0.2C.

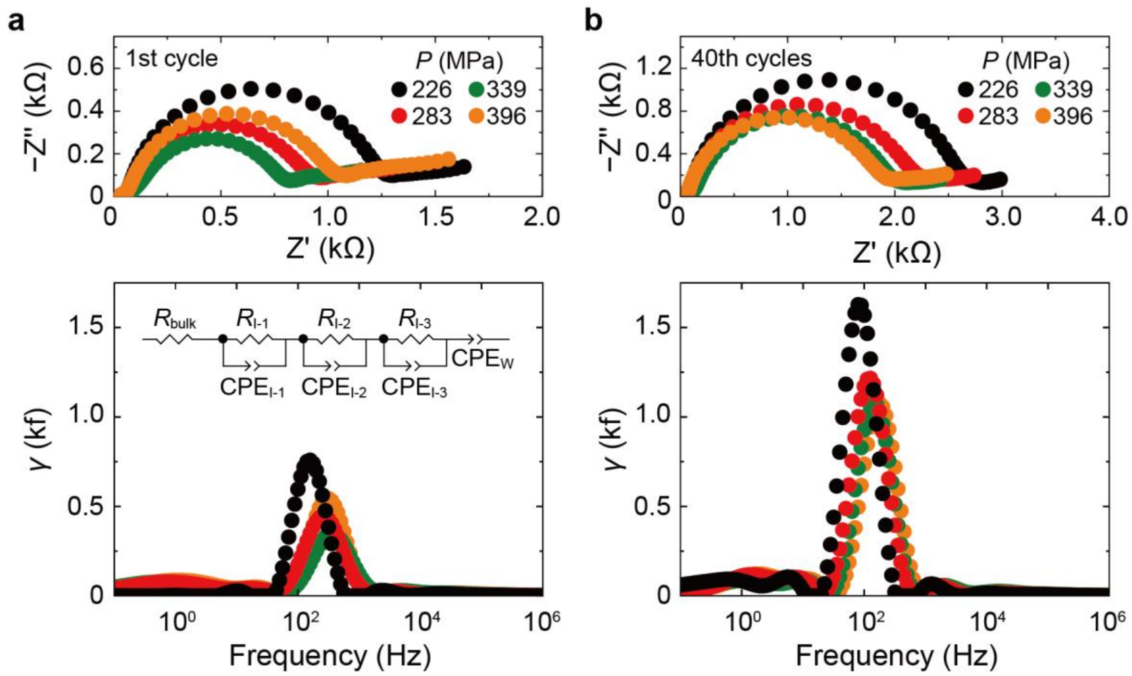

Fig. S4. Electrochemical impedance spectroscopy (EIS) analysis of FUPCs. Nyquist plot and distribution of relaxation times (DRT) curves for the FUPCs at (a) 1 cycle and (b) 40 cycles.

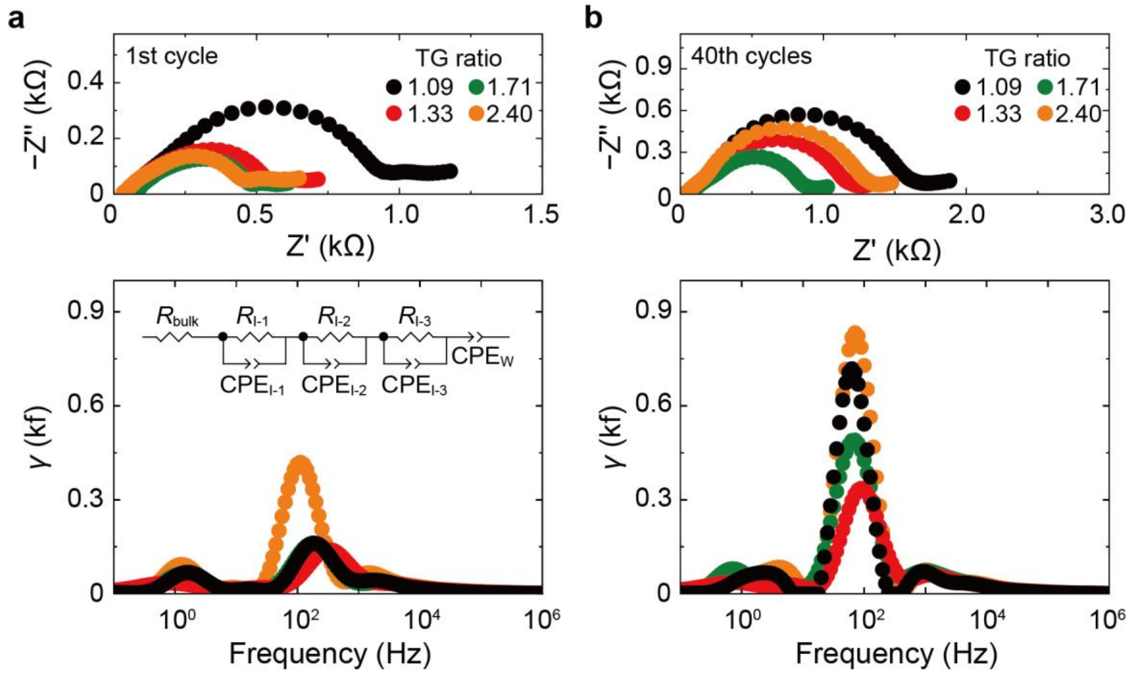

Fig. S5. EIS analysis of RUPCs. Nyquist plot and DRT curves for the RUPCs at (a) 1 cycle and (b) 40 cycles.

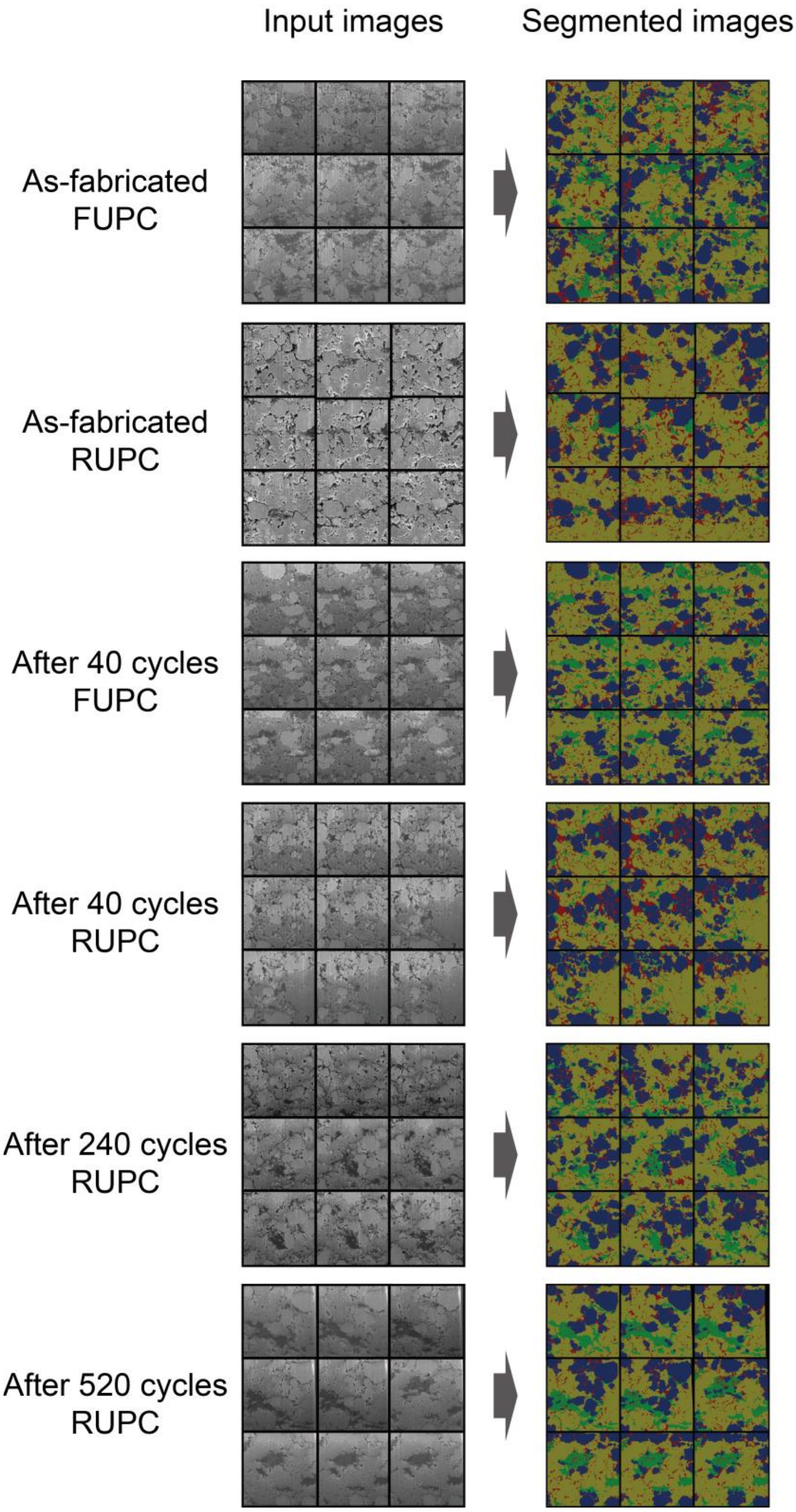

Fig. S6. Input and segmented images included the as-fabricated and after cycle states of FUPCs and RUPCs, and after a long-cycling test of RUPCs.

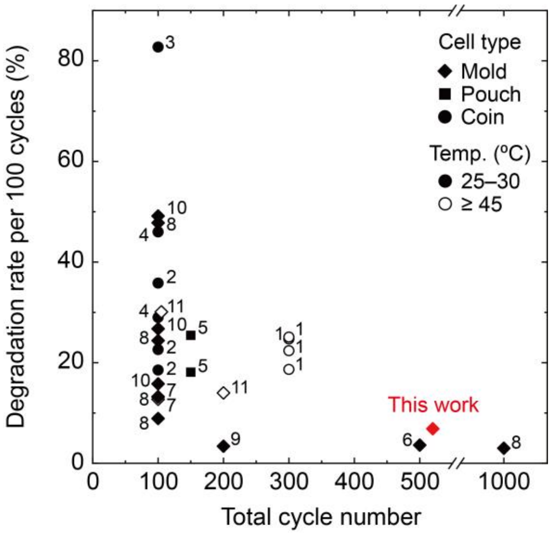

Fig. S7. Comparison of the degradation rates in this work with those of previously reported cells [wet-cast and sulfide-based solid electrolytes (SEs)].[1–11] Open and solid symbols indicate cell-operating temperature of ≥ 45 °C and around room temperature (25–30 °C), respectively.

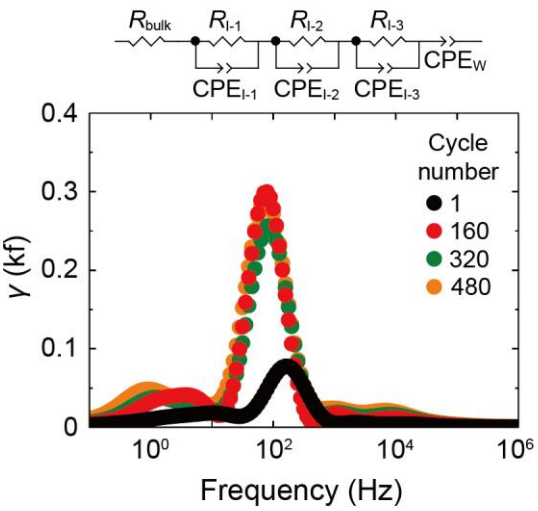

Fig. S8. DRT curves of RUPCs under a long-cycling test.

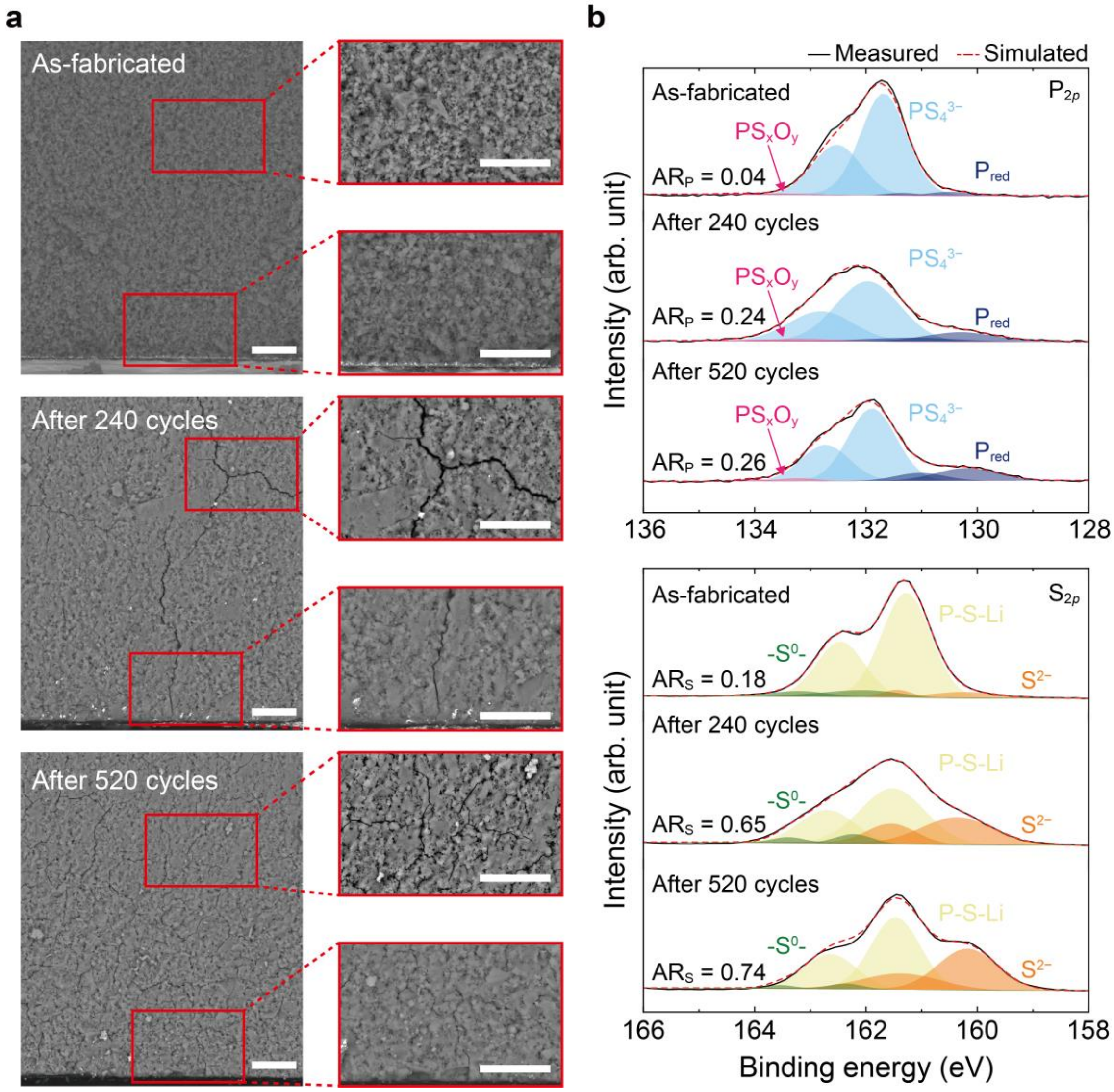

Fig. S9. Scanning electron microscope (SEM) images and X-ray photoelectron spectroscopy (XPS) results of RUPCs. (a) SEM images of the electrolyte layer and electrolyte-anode interface on RUPCs showing the microstructural evolution for as-fabricated (top), after 240 (middle), and 520 (bottom) cycles. All scale bars correspond to 5 μm. (b) XPS spectra of P_{2p} and S_{2p} elements of the electrolyte-anode interface for as-fabricated, 240-, and 520-cycled conditions. The XPS results showed significant growth of peaks (*e.g.*, PS_xO_y, P_{red}, -S^0-, and S^{2-}) representing the decomposition products for each material. The area ratio (AR_i, where *i* is P or S) of decomposition reactions is given by the grown decomposition product to that of the pristine constituent in element *i*.

Table S1. Quantitative parameters including phase fraction, interconnectivity, and double-phase boundary (DPB) density. CAM and ECM indicate cathode active material and electronic conductive material.

Material	Phase fraction (%)				Interconnectivity				DPB density (μm^{-1})			
	CAM	SE	ECM	Pore	CAM	SE	ECM	Pore	CAM-ECM	SE-ECM	CAM-ECM	Others
Uncycled FUPCs	27.41	49.98	11.87	10.74	0.178	0.407	0.136	0.280	0.563	0.074	0.444	1.638
Uncycled RUPCs	27.53	55.12	9.98	7.36	0.200	0.422	0.133	0.246	0.616	0.062	0.414	1.252
40-cycled FUPCs	27.48	56.87	3.63	12.02	0.153	0.444	0.067	0.336	0.394	0.026	0.206	1.645
40-cycled RUPCs	31.90	52.25	4.24	11.58	0.191	0.436	0.083	0.290	0.469	0.047	0.304	1.407
240-cycled RUPCs	30.57	52.56	9.53	7.33	0.218	0.417	0.142	0.222	0.532	0.116	0.462	1.021
520-cycled RUPCs	26.74	52.38	12.69	6.66	0.192	0.384	0.168	0.257	0.330	0.102	0.338	1.074

Table S2. Comparison of quantitative parameters with experimental values.

Material	Phase fraction (%)		
	CAM	SE	ECM
Experimental value	35.76	58.87	5.36
Uncycled FUPCs	30.68	55.99	13.33
Uncycled RUPCs	29.70	59.50	10.80
40-cycled FUPCs	31.25	64.66	4.09
40-cycled RUPCs	36.09	59.16	4.75
240-cycled RUPCs	33.01	56.74	10.25
520-cycled RUPCs	29.08	57.08	13.83
Average	31.64	58.86	9.51

Table S3. Comparison of the electrochemical performance and degradation rate in this work with that of previously reported papers (wet-cast and sulfide-based SEs).

Ref.	Cell type	Total cycle number	C-rate	Temp. (°C)	Initial Discharge capacity (mAh g^{-1})	Final Discharge capacity (mAh g^{-1})	Retention (%)	Degradation rate per 100 cycles (%)
1	Coin	300	1C	60	67.28	29.60	44.00	18.67
1	Coin	300	1C	60	63.34	16.36	25.83	24.72
1	Coin	300	1C	60	60.00	19.70	32.83	22.39
1	Coin	300	1C	60	57.58	14.24	24.73	25.09
2	Coin	100	0.1C	R.T.	127.50	81.82	64.17	35.83
2	Coin	100	0.1C	R.T.	114.70	93.44	81.46	18.54
2	Coin	100	0.1C	R.T.	136.30	105.50	77.40	22.60
3	Coin	100	0.02C	25	124.18	21.43	17.26	82.74
4	Coin	100	0.02C	30	130.00	92.30	71.00	29.00
4	Coin	100	0.05C	30	96.08	51.88	54.00	46.00
5	Pouch	150	0.2C	30	153.00	111.39	72.80	18.13
5	Pouch	150	0.2C	30	121.00	74.78	61.80	25.47
6	Mold	500	0.5C	25	180.22	129.00	71.58	3.62
7	Mold	100	0.5C	25	61.00	52.92	86.75	13.25
7	Mold	100	0.5C	60	120.17	104.88	87.28	12.72
8	Mold	100	0.64C	25	162.35	147.90	91.10	8.90
8	Mold	100	0.64C	25	154.23	116.60	75.60	24.40
8	Mold	100	0.64C	25	134.68	116.90	86.80	13.20
8	Mold	100	0.64C	25	130.08	67.90	52.20	47.80
8	Mold	1000	0.64C	25	146.61	102.72	70.06	2.99
9	Mold	200	0.5C	30	160.00	149.12	93.20	3.40
10	Mold	100	0.2C	25	150.80	76.67	50.84	49.16
10	Mold	100	0.2C	25	148.33	124.89	84.20	15.80
10	Mold	100	0.2C	25	142.20	104.17	73.26	26.74
11	Mold	200	0.5C	60	189.69	136.58	72.00	14.00
11	Mold	105	0.5C	60	180.90	123.71	68.39	30.11
This work	Mold	520	0.2C	25	149.32	95.96	64.26	6.87

Table S4. Individual fitting component (R, CPE-T, CPE-P, and C) values obtained from EIS curves by conventional fitting method of FUPCs after 1 and 40 cycles.

Pressure (MPa)	FUPCs after 1 cycle			
	226	283	339	396
R_{bulk} (Ω)	40.51	35.02	55.55	39.82
R_{I-1} (Ω)	33.4	43.06	76.25	34.44
CPE-T_{I-1} ($Fs^{\alpha-1}$)	1.3882E−5	2.3473E−5	2.1577E−5	2.4211E−5
CPE-P_{I-1} (α)	0.64735	0.56222	0.55027	0.576
C_{I-1} (F)	2.12E−7	1.09E−7	1.15E−7	1.30E−7
R_{I-2} (Ω)	1136	810.2	642	908.2
CPE-T_{I-2} ($Fs^{\alpha-1}$)	1.67E−6	2.1278E−6	2.0935E−6	1.3924E−6
CPE-P_{I-2} (α)	0.911	0.85994	0.85618	0.88255
C_{I-2} (F)	9.04E−7	7.55E−7	6.89E−7	5.73E−7
R_{I-3} (Ω)	356.8	385.1	407.3	430
CPE-T_{I-3} ($Fs^{\alpha-1}$)	1.13E−3	1.0739E−3	1.2183E−3	7.9396E−4
CPE-P_{I-3} (α)	0.605	0.57405	0.55508	0.5749
C_{I-3} (F)	6.21E−4	5.58E−4	6.95E−4	3.59E−4
Pressure (MPa)	**FUPCs after 40 cycles**			
	226	283	339	396
R_{bulk} (Ω)	45.86	44.04	64.27	39.86
R_{I-1} (Ω)	43.82	50.33	90.53	34.44
CPE-T_{I-1} ($Fs^{\alpha-1}$)	2.5197E−5	1.2598E−5	1.3091E−5	2.4074 E−5
CPE-P_{I-1} (α)	0.56901	0.62084	0.59557	0.5829
C_{I-1} (F)	1.45E−7	1.40E−7	1.35E−7	1.50E−7
R_{I-2} (Ω)	2459	2016	1726	1713
CPE-T_{I-2} ($Fs^{\alpha-1}$)	1.372E−6	1.3933E−6	1.314E−6	1.0964E−6
CPE-P_{I-2} (α)	0.90904	0.88565	0.89398	0.89515
C_{I-2} (F)	7.76E−7	6.53E−7	6.38E−7	5.26E−7
R_{I-3} (Ω)	471.8	418.9	427.6	461.7
CPE-T_{I-3} ($Fs^{\alpha-1}$)	1.1522E−3	5.045E−4	6.9294E−4	4.1648E−4
CPE-P_{I-3} (α)	0.54421	0.66839	0.57069	0.64856
C_{I-3} (F)	6.92E−4	2.33E−4	2.78E−4	1.70E−4

Table S5. Individual fitting component values obtained from EIS curves by conventional fitting method of RUPCs after 1 and 40 cycles

TG ratio	RUPCs after 1 cycle			
	1.09	1.33	1.71	2.40
R_{bulk} (Ω)	34.64	65.71	43.09	47.87
R_{I-1} (Ω)	197.5	201.7	199.6	200.4
CPE-T$_{I-1}$ ($Fs^{\alpha-1}$)	2.98E−5	6.37E−5	2.10E−5	1.55E−5
CPE-P$_{I-1}$ (α)	0.58904	0.50136	0.61899	0.63206
C_{I-1} (F)	8.30E-07	8.37E-07	7.22E-07	5.36E-07
R_{I-2} (Ω)	228.9	219.1	310.8	677.8
CPE-T$_{I-2}$ ($Fs^{\alpha-1}$)	8.72E−6	7.47E−6	9.30E−6	4.50E−6
CPE-P$_{I-2}$ (α)	0.8847	0.84479	0.83328	0.88516
C_{I-2} (F)	3.88E-06	2.30E-06	2.89E-06	2.12E-06
R_{I-3} (Ω)	126.1	119.3	109.5	151
CPE-T$_{I-3}$ ($Fs^{\alpha-1}$)	1.11E−3	2.94E−3	1.48E−3	1.03E−3
CPE-P$_{I-3}$ (α)	0.84937	0.66914	0.86853	0.88648
C_{I-3} (F)	7.87E-04	1.75E-03	1.12E-03	8.08E-04
TG ratio	RUPCs after 40 cycles			
	1.09	1.33	1.71	2.40
R_{bulk} (Ω)	39.27	65.65	51.1	55.85
R_{I-1} (Ω)	198.9	212.5	205.7	202.9
CPE-T$_{I-1}$ ($Fs^{\alpha-1}$)	1.85E−5	2.19E−5	1.34E−5	1.56E−5
CPE-P$_{I-1}$ (α)	0.61077	0.59188	0.646	0.61142
C_{I-1} (F)	5.19E−7	5.38E−7	5.31E−7	4.02E−7
R_{I-2} (Ω)	1005	572.9	910.1	1257
CPE-T$_{I-2}$ ($Fs^{\alpha-1}$)	3.94E−6	7.18E−6	6.32E−6	3.12E−6
CPE-P$_{I-2}$ (α)	0.92525	0.86795	0.853	0.90741
C_{I-2} (F)	2.52E−6	3.11E−6	2.61E−6	1.77E−6
R_{I-3} (Ω)	147.4	132.2	124.9	188.6
CPE-T$_{I-3}$ ($Fs^{\alpha-1}$)	8.12E−4	2.89E−3	2.09E−3	7.41E−4
CPE-P$_{I-3}$ (α)	0.83444	0.64732	0.891	0.75471
C_{I-3} (F)	5.33E−4	1.71E−3	1.77E−3	3.91E−4

Table S6. Individual fitting component values obtained from EIS curves by conventional fitting method of RUPCs under a long-cycling test.

Cycle number	RUPCs under a long-cycling test			
	1	160	320	480
R_{bulk} (Ω)	30.23	94.84	144.3	193.4
R_{I-1} (Ω)	12.54	37.97	50.08	65.71
CPE-T_{I-1} ($Fs^{\alpha-1}$)	3.31E−5	1.86E−5	1.21E−5	1.07E−5
CPE-P_{I-1} (α)	0.6904	0.66816	0.68598	0.6823
C_{I-1} (F)	1.01E−6	5.06E−7	4.09E−7	3.62E−7
R_{I-2} (Ω)	139.2	518.3	508.7	608.4
CPE-T_{I-2} ($Fs^{\alpha-1}$)	1.92E−5	8.75E−6	1.03E−5	1.03E−5
CPE-P_{I-2} (α)	0.85154	0.8735	0.83795	0.82279
C_{I-2} (F)	6.84E−6	4.00E−6	3.72E−6	3.45E−6
R_{I-3} (Ω)	86.16	125.8	118.3	151.5
CPE-T_{I-3} ($Fs^{\alpha-1}$)	1.67E−3	1.36E−3	1.96E−3	1.94E−3
CPE-P_{I-3} (α)	0.54071	0.69945	0.70367	0.69958
C_{I-3} (F)	3.21E−4	6.39E−4	1.06E−3	1.15E−3

Table S7. Detailed Resistance values obtained from DRT method in FUPCs and RUPCs.

Pressure (MPa)	FUPCs after 1 cycle			
	226	283	339	396
R_{bulk} (Ω)	40.51	35.02	55.55	39.82
R_{I-1} (Ω)	27.85	335.39	364.79	436.63
R_{I-2} (Ω)	1463.27	728.36	564.23	904.87
R_{I-3} (Ω)	35.08	174.61	196.54	31.14
Pressure (MPa)	FUPCs after 40 cycles			
	226	283	339	396
R_{bulk} (Ω)	45.86	44.04	64.27	39.86
R_{I-1} (Ω)	463.29	443.91	440.31	464.23
R_{I-2} (Ω)	2454.30	1982.69	1737.72	1698.35
R_{I-3} (Ω)	57.03	58.63	66.10	46.56
TG ratio	RUPCs after 1 cycle			
	1.09	1.33	1.71	2.40
R_{bulk} (Ω)	34.64	65.71	43.09	47.87
R_{I-1} (Ω)	123.76	112.61	119.40	161.96
R_{I-2} (Ω)	202.39	189.81	252.80	698.12
R_{I-3} (Ω)	226.35	237.68	247.70	169.12
TG ratio	RUPCs after 40 cycles			
	1.09	1.33	1.71	2.40
R_{bulk} (Ω)	39.27	65.65	51.1	55.85
R_{I-1} (Ω)	138.31	156.69	144.41	187.46
R_{I-2} (Ω)	1063.01	555.49	877.16	1291.85
R_{I-3} (Ω)	149.98	205.42	219.13	169.19
Cycle number	RUPCs under a long-cycling test			
	1	160	320	480
R_{bulk} (Ω)	30.23	94.84	144.3	193.4
R_{I-1} (Ω)	91.89	129.46	137.55	179.41
R_{I-2} (Ω)	124.17	497.92	458.97	536.27
R_{I-3} (Ω)	21.84	54.68	80.56	109.93

References

1. J. Zhang, H. Zhong, C. Zheng, Y. Xia, C. Liang, H. Huang, Y. Gan, X. Tao, and W. Zhang, *J. Power Sources*, 2018, **391**, 73–79.
2. Q. Ye, X. Li, W. Zhang, Y. Xia, X. He, H. Huang, Y. Gan, X. Xia, and J. Zhang, *ACS Appl. Mater. Interfaces*, 2023, **15**, 18878–18888.
3. S. Choi, M. Jeon, J. Ahn, W. D. Jung, S. M. Choi, J. -S. Kim, J. Lim, Y. -J. Jang, H. -G. Jung, J. -H. Lee, B. -I. Sang, and H. Kim, *ACS Appl. Mater. Interfaces*, 2018, **10**, 23740–23747.
4. Y. Xia, J. Li, Z. Xiao, X. Zhou, J. Zhang, H. Huang, Y. Gan, X. He, and W. Zhang, *ACS Appl. Mater. Interfaces*, 2022, **14**, 33361–33369.
5. T. Y. Kwon, K. T. Kim, D. Y. Oh, Y. B. Song, S. Jun, and Y. S. Jung, *Energy Stor. Mater.*, 2022, **49**, 219–226.
6. S. Jing, H. Shen, Y. Huang, W. Kuang, Z. Zhang, S. Liu, S. Yin, Y. Lai, and F. Liu, *Adv. Funct. Mater.*, 2023, **33**, 2214274.
7. D. Lee, Y. Shim, Y. Kim, G. Kwon, S. H. Choi, K. Kim, and D. -J. Yoo, *Nat. Commun.*, 2024, **15**, 4763.
8. J. Gao, J. Hao, Y. Gao, X. Sun, Y. Zhang, D. Song, Q. Zhao, F. Zhao, W. Si, K. Wang, T. Ohsaka, F. Matsumoto, J. Wu, and H. Xie, *eTransportation*, 2023, **17**, 100252.
9. K. T. Kim, T. Y. Kwon, Y. B. Song, S. -M. Kim, S. C. Byun, H. -S. Min, S. H. Kim, and Y. S. Jung, *J. Chem. Eng.*, 2022, **450**, 138047.
10. Y. -J. Lee, S. -B. Hong, and D. -W. Kim, *J. Ind. Eng. Chem.*, 2023, **122**, 341–348.
11. S. -B. Hong, Y. -R. Jang, Y. -C. Jung, W. Cho, and D. -W. Kim, *ACS Appl. Energy Mater.*, 2024, **7**, 5193–5201.